ELSEVIER

Mathematical Model of Erythrocytes as Point-Like Sources

CEES BOS AND LOUIS HOOFD
Department of Physiology

AND

THOM OOSTENDORP
Department of Medical Physics and Biophysics
University of Nijmegen, PO Box 9101, 6500 HB Nijmegen, The Netherlands

Received 30 May 1993; revised 28 April 1994

ABSTRACT

A new approach to investigate the effect of pericapillary gradients, caused by the particulate nature of blood, on oxygen partial pressure (pO_2) in tissue is presented. The blood erythrocytes are modeled as point-like sources, which makes the system independent of the geometry of the erythrocytes. This model is semi-analytical and is developed to estimate the pO_2 far from the erythrocytes. It does so through calculation of the extraction pressure, which accounts for the capillary oxygen drop as compared to homogeneous blood. It is particularly useful to estimate pO_2 in regions where the oxygen concentration is low.

Simulations have been performed for a cylindrical tissue geometry and parameters are chosen for rat heart muscle. In accordance with the literature, for a fixed total oxygen supply low hematocrit values result in a lower pO_2 at the border of the tissue cylinder than high values do. Also a decrease in hematocrit results in higher values for the extraction pressure. Finally, it was found that the effect of the particulate nature of blood is most distinct at low hematocrit values.

INTRODUCTION

Modeling of oxygen transport to tissue is often based on the Krogh model [15]. Although this model uses numerous assumptions, some of them being quite unrealistic [14], it is still useful as a basis for comparison and investigation of effects of parameter modifications [10]. On the other hand, numerical non-steady-state approaches are time-consuming and therefore limited in their possibilities. As a result, there is a need for a fast (semi-) analytical solution. The physiologically most interest-

MATHEMATICAL BIOSCIENCES 125:165–189 (1995)

655 Avenue of the Americas, New York, NY 10010 0025-5564/95/$9.50
SSDI 0025-5564(94)00026-V

ing aspect of the modeling of oxygen transfer to tissue is estimation of the number and size of regions where the oxygen concentration is low. Those regions will normally be at some distance from the capillaries. In this case a model is needed that is accurate at least at distant locations from the capillaries.

For the Krogh approach a number of mathematical extensions were developed, as a result of which it has a much broader applicability [6, 10, 16]. The most important remaining problem is that of pericapillary gradients, which determine the oxygen level for further oxygen diffusion in and into the tissue. Some studies already showed that these gradients can be of major importance [1, 2, 5, 7–10, 18, 19]. Different approaches and methods on oxygen transport are reviewed in the literature [17].

In this study, a model is presented to estimate the effect of pericapillary gradients caused by the particulate nature of blood on the partial oxygen pressure (pO_2) further into the tissue. The estimate, a simple factor, can be used to correct the assumption of a continuous distribution of oxygen in the capillary. This is investigated in detail in the layout of the Krogh cylinder. There exist previous studies on the effect of the particulate nature of blood on the tissue pO_2 [1, 2, 4, 5, 7–9, 22]. However, since the present model aims at the pO_2 estimation at distant locations, additional assumptions can be made which speed up the calculation and eventually lead to direct formulas for estimating distant pO_2 drop. This distant pO_2 drop is caused by plain oxygen diffusion in the tissue on the one hand and by the particulate nature of the blood on the other hand. The latter pO_2 drop is called the extraction pressure (EP).

A value of zero for the EP can be considered as the zero-order approximation. A first-order approximation is presented here, which determines the maximum effect of the particulate nature of blood and therefore can be considered as a worst-case approximation. In order to derive a first-order approximation, the geometry of the erythrocytes is not considered, and the erythrocyte as an oxygen source is kept as simple as possible, point-like oxygen sources. This source must be located to mimic erythrocyte oxygen release. The location does not necessarily coincide with the center of the erythrocytes. The analytical solution for point-like sources is well known, e.g., from electromagnetism.

The model presented here is based on the following phenomena: oxygen diffusion, binding of oxygen to myoglobin in the tissue, binding of oxygen to hemoglobin in the erythrocyte, a constant rate of oxygen consumption, quasi-steady-state, and erythrocytes as point-like sources. It is used to simulate the oxygen transfer in rat heart muscle. Data used here are for rat heart muscle. Muscle tissue is modeled as a cylinder of

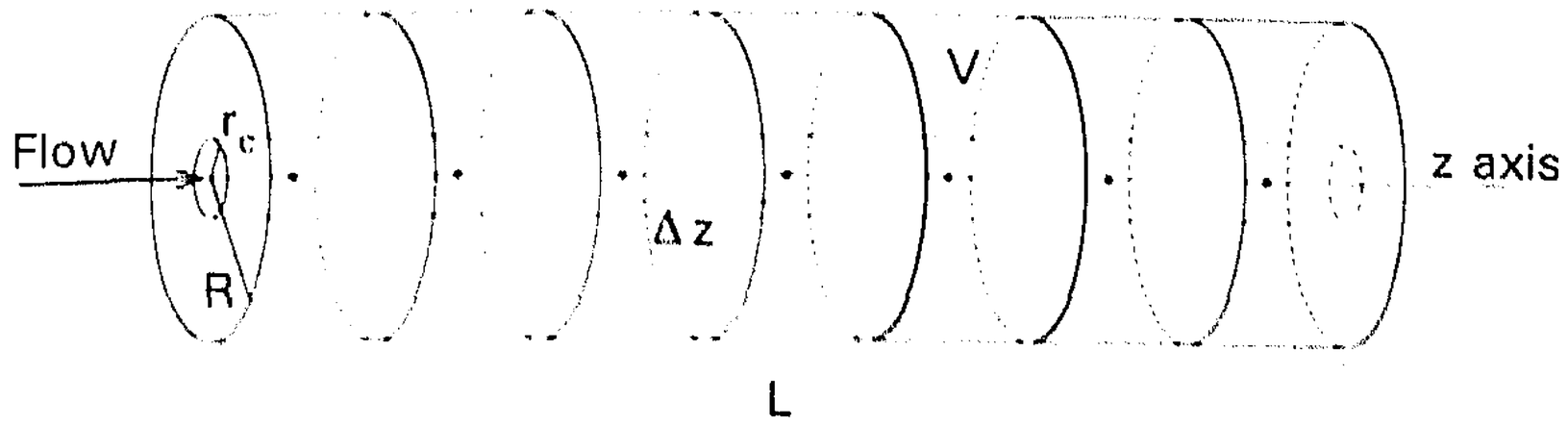

FIG. 1. Geometry used for the model. R denotes the tissue cylinder radius, L the length, V the total volume of erythrocyte, plasma and tissue supplied by one erythrocyte, r_c the capillary radius and Δz the distance between the midpoint of two successive erythrocytes.

homogeneous tissue, ignoring possible tissue heterogeneities [3]. The capillary array of erythrocytes is treated as a series of sources each supplying an equally sized tissue volume V_t and the erythrocytes are equally spaced (constant distance Δz). The system is defined in such a way that—as if a stroboscope was used—at every time instant $t = t_0 + i\,\Delta t$, exactly the same situation exists, where i is an integer number.

MATHEMATICAL REPRESENTATION

ASSUMPTIONS AND BASIC EQUATIONS

As shown in Figure 1, the tissue cylinder has radius R and length L. The axis of the cylinder is the z axis which runs from $-L/2$ to $L/2$. The capillary is situated at the center of the cylinder and has radius r_c. In order to use a stroboscopic approach, all erythrocytes have to be spaced equally, and hence they all support an equally large volume V. In line with the chosen geometry, cylindrical coordinates are used such that $\vec{r} = (r, \phi, z)$. The erythrocytes are at the locations $\vec{r}_i = (0, 0, z_i)$ and z_i is set to $-L/2 + (i - \frac{1}{2})\Delta z$ with $\Delta z = L/N$, where Δz is the distance between two successive erythrocytes, N is the number of erythrocytes, and i is the erythrocyte index ($1 \leqslant i \leqslant N$).

In the present model the following major assumptions are:

1. The geometry of the tissue supplied by this capillary is a cylinder.
2. The oxygen consumption is described by zero-order kinetics.
3. All the erythrocytes are equally spaced and move with constant speed.
4. The erythrocytes can be modeled as point-like sources.
5. The boundary conditions for the erythrocytes are those of a sphere of the same volume.

6. The oxygen transport properties of the capillary content outside the erythrocytes are identical to the oxygen transport properties of the tissue.

7. A stroboscope approach can be used, where the system reaches the same state in an interval Δt in which the erythrocytes travel the distance Δz between the erythrocytes.

Some of these assumptions are discussed in the literature [10, 14], but assumptions (4) to (7) need some additional explanation.

The modeling of erythrocytes as point-like sources is unrealistic, but not the only unrealistic way of modeling. Wang and Popel [22] showed that the geometry of the erythrocytes can play an important role in the oxygen transport. Therefore, also when erythrocytes are modelled as 'simple' cylinders or spheres, the mismatch of the calculated pO_2 gradients and the in vivo pO_2 gradients can be considerable. One of the possibilities to avoid this problem is to consider the pO_2 at a relatively large distance from the erythrocytes since the influence of the geometry decreases with increasing distance. At locations sufficient far from the erythrocyte no distinction can be made between a real erythrocyte and a point-like source.

The problem of modeling the erythrocytes as point-like sources is that no realistic boundary conditions can be applied. However, when an erythrocyte is modeled as a sphere, outside the sphere the oxygen transport is identical to that of a point-like source. Then, also as a first-order approximation, a boundary condition can be imposed equalling the erythrocytic pO_2 to that at the surface of the sphere. The sphere boundary condition is not related to the actual form of the erythrocyte. Actual erythrocyte form is uncertain in realistic capillaries and is modeled in different ways in the literature, often cylindrical but also ellipsoidal or 'parachute-like.' Since the spherical shape is a fictitious one the spheres do not have to fit the capillary and the sphere radius r_E is not equal to the capillary radius r_c.

Since we are interested only in the effect of separate sources instead of a homogeneous source the plasma is not taken into account and a model is used where the sources are surrounded by a medium with the same properties as the tissue. This will of course result in a different resistance to oxygen transport in the capillary region than if plasma were incorporated in the model. Note that in the calculations the pO_2 in the capillary is so high that myoglobin does not play a role in the capillary and that the plasma volume is small compared to the tissue volume. The extraction pressure calculated with this model accounts only for the effect of discrete sources. A more sophisticated model will need an additional calculation of the differences in the oxygen transport between tissue and plasma.

The stroboscope approach must be considered as a first-order approach. It will be a valid model in the limiting case of stagnant erythrocytes. Therefore for low erythrocyte velocities this approach is likely to result in good approximations. A more quantitative motivation for the use of the stroboscope approach is considered in Appendix A.

In tissue the oxygen transport is determined by the diffusion of oxygen and the diffusion of oxymyoglobin. The equations describing diffusion and consumption are given below for a static frame. The flux based on the diffusion of oxygen ($\vec{J}_{O_2}$) is:

$$\vec{J}_{O_2} = -\mathscr{P}\vec{\nabla}p, \tag{1}$$

where p is oxygen partial pressure, $\mathscr{P}$ is the oxygen permeability constant, and ∇ is the gradient operator. The flux of oxymyoglobin ($\vec{J}_{O_2Mb}$) is described by:

$$\vec{J}_{O_2Mb} = -D_{O_2Mb}\vec{\nabla}c_{O_2Mb}, \tag{2}$$

where D_{O_2Mb} is the oxymyoglobin diffusion constant, and c_{O_2Mb} is the concentration of oxymyoglobin. Now the total oxygen flux can be written as

$$\vec{J} = \vec{J}_{O_2} + \vec{J}_{O_2Mb} \tag{3}$$

Based on mass balance the following nonsteady-state equation can be derived:

$$\frac{\partial c_{O_2}}{\partial t} + \vec{\nabla}\cdot\vec{J} = -\dot{Q}, \tag{4}$$

where $\dot{Q}$ is the oxygen consumption, c_{O_2} is the total amount of oxygen per volume, and t is the time. Since steady-state is assumed, $\partial c_{O_2}/\partial t = 0$, and if $\mathscr{P}$ is homogeneous, (3) and (4) can be combined to

$$\mathscr{P}\nabla^2 p^* = \dot{Q}, \tag{5}$$

where p^* drives the diffusion. If the diffusivity of myoglobin and oxymyoglobin are identical, the myoglobin facilitation can be modeled

by [10]:

$$p^* = p + p_F s_{Mb}; \qquad s_{Mb} = \frac{c_{O_2Mb}}{c_{Mb} + c_{O_2Mb}} = \frac{p}{p_{50,Mb} + p}, \tag{6}$$

where s_{Mb} is the myoglobin saturation, $p_F = D_{O_2Mb}(c_{Mb} + c_{O_2Mb})/\mathscr{P}$ is the facilitation pressure, and $p_{50,Mb}$ is the pO_2 at which the myoglobin is 50% saturated.

Within the erythrocytes the binding of oxygen to hemoglobin is assumed to follow Hill's equation, which states for the saturation (s)

$$s = \frac{p^n}{p^n + p_{50}^n}, \tag{7}$$

where n is the Hill coefficient and p_{50} is the pO_2 at which the hemoglobin is 50% saturated. This equation adequately describes the oxygen binding curve for saturation values higher than about 10%.

OXYGEN LOSS OF ERYTHROCYTES

In the stroboscope approach we need to consider the time Δt in which the erythrocytes travel a distance Δz. The oxygen loss of the erythrocytes and the intermediate plasma is equal to the total amount of oxygen consumed in a certain tissue volume V_T. The actual location of this tissue volume is not relevant. From Figure 1 it might be inferred that V_T is coincident with $V - \pi r_c^2 \Delta z$, but that volume also receives oxygen from other sources while oxygen from the adjacent source diffuses to other cylinder slices. The volume of V_T is numerically equal to $V - \pi r_c^2 \Delta z$, but the shape and location are not defined here. Within the subsequent discretization steps the oxygen loss can be defined as

$$n_{i+1} - n_i = -\Delta t \dot{Q} V_T = -\frac{\Delta z}{v} \dot{Q} V_T, \tag{8}$$

where n_i is the oxygen contained in the plasma and the erythrocyte in and around erythrocyte i, and v is the velocity of the erythrocytes. The total amount of oxygen in erythrocyte i is

$$c_{E,i} = c_{Hm} s_i + \alpha_E p_{E,i}, \tag{9}$$

where c_{Hm} is the oxygen binding capacity, which is equal to the heme concentration (four times hemoglobin concentration), s_i is the oxygen saturation of hemoglobin in erythrocyte i, α_{E} is the oxygen solubility inside the erythrocyte, and $p_{\mathrm{E},i}$ the pO_2 inside erythrocyte i. The total amount of oxygen in both the erythrocyte and its surrounding plasma volume is

$$n_i = (c_{\mathrm{Hm}} s_i + \alpha_{\mathrm{E}} p_{\mathrm{E},i}) V_{\mathrm{E}} + \alpha_{\mathrm{p}} p_{\mathrm{p},i} V_{\mathrm{p}}, \tag{10}$$

where α_{p} is the oxygen solubility in the plasma, V_{p} is the plasma volume assigned to the erythrocyte with volume V_{E}, and $p_{\mathrm{p},i}$ the mean pO_2 in the plasma. We assume that the difference $\Delta p_{\mathrm{E,p}} = \mathrm{p}_{\mathrm{E},i} - \mathrm{p}_{\mathrm{p},i}$ is a constant. This assumption is valid when $\alpha_{\mathrm{p}} p_{\mathrm{p},i} V_{\mathrm{p}}$ is small compared to $n_{i+1} - n_i$. Note that $\alpha_{\mathrm{p}} p_{\mathrm{p},i} V_{\mathrm{p}}$ itself is a small fraction of n_i. Thus it can be derived that

$$c_{\mathrm{Hm}} V_{\mathrm{E}} (s_{i+1} - s_i) + (\alpha_{\mathrm{E}} V_{\mathrm{E}} + \alpha_{\mathrm{p}} V_{\mathrm{p}})(p_{\mathrm{E},i+1} - p_{\mathrm{E},i}) = -\dot{Q} V_{\mathrm{T}} \frac{\Delta z}{v}. \tag{11}$$

The sum of erythrocyte volume and plasma volume can be replaced by

$$\pi r_{\mathrm{c}}^2 \Delta z = V_{\mathrm{E}} + V_{\mathrm{p}} \tag{12}$$

and the tissue volume V_{T} can be substituted by

$$V_{\mathrm{T}} = V - (V_{\mathrm{E}} + V_{\mathrm{p}}) = \pi (R^2 - r_{\mathrm{c}}^2) \Delta z. \tag{13}$$

The blood flow F and the capillary hematocrit H are introduced by

$$F = \pi r_{\mathrm{c}}^2 v \tag{14}$$

$$V_{\mathrm{E}} = H(V_{\mathrm{E}} + V_{\mathrm{p}}) = H \pi r_{\mathrm{c}}^2 \Delta z. \tag{15}$$

With these substitutions, (11) can be transformed to

$$c_{\mathrm{Hm}} H (s_{i+1} - s_i) + \{\alpha_{\mathrm{p}} + (\alpha_{\mathrm{E}} - \alpha_{\mathrm{p}}) H\}(p_{\mathrm{E},i+1} - p_{\mathrm{E},i}) = -\frac{\pi \dot{Q} (R^2 - r_{\mathrm{c}}^2) \Delta z}{F}. \tag{16}$$

This can be interpreted as a discrete version of the formulas used by Klitzman et al. [13]. They developed a continuum treatment to obtain boundary conditions for the tissue oxygenation describing differential equations. Since s and p_{E} are related, all $p_{\mathrm{E},i}$ can be determined when

the pO_2 of the first erythrocyte is known. As a starting condition for $p_{E,1}$ the arteriolar pO_2, p_a is used.

SPHERICAL SYMMETRIC SOLUTION

The cylindrical solution is derived from the spherical symmetric solution for one point source in a large homogeneous tissue unit. In a sphere, the spherical coordinate system is used, defined as $\vec{r} = (\rho, \theta, \phi)$ with the origin at the point-like source. Because of spherical symmetry, only the distance ρ from the center has to be considered and the angles θ and ϕ can be omitted. This results in the following Laplace operator:

$$\nabla^2 = \frac{1}{\rho^2}\frac{\partial}{\partial\rho}\left(\rho^2\frac{\partial}{\partial\rho}\right) = \frac{\partial^2}{\partial\rho^2} + \frac{2}{\rho}\frac{\partial}{\partial\rho}. \tag{17}$$

When the general solution to (5) is integrated using this Laplace operator and with the condition of no flux at the rim of the spherical support volume of size $V = V_T + V_E + V_p$, it can be derived that

$$p^*(\rho) = p_0^* + \frac{\dot{Q}}{4\mathscr{P}}\left\{\frac{2}{3}\rho^2 + \frac{V}{\pi\rho}\right\}, \tag{18}$$

where p_0^* is an integration constant. The term $(\dot{Q}/4\mathscr{P})(V/\pi\rho)$ can be interpreted as the contribution of the source and $(\dot{Q}/4\mathscr{P})(2\rho^2/3)$ as the contribution of the surrounding consuming tissue.

GENERALIZED SOLUTION

The spherical solution can be extended to a general solution. To do so, the three parts of (18) have to be qualified and transformed into a general representation. The generalized solution will be presented independent of the geometry, which implies that the equations will be in terms of the vector $\vec{r}$. The three parts will be transformed as follows:

- The contribution of surrounding tissue $(\dot{Q}/4\mathscr{P})(2\rho^2/3)$ depends on the geometry of the system and is specific for the spherical solution. The generalized form of $2\rho^2/3$ is denoted by $\Phi(\vec{r})$ and will be called the field term. This field term depends on the boundary conditions and will be specified later.
- The source term $V/(\pi\rho)$ can be written as $V/(\pi|\vec{r} - \vec{r}_i|)$ where $\vec{r}_i$ is the location of erythrocyte i. In a general system there will be N erythrocytes and the total contribution of the sources will be the sum of the particulate contributions.
- p_0^* can be interpreted as a general level of pO_2 and will be accounted for in the field term.

Now the generalized solution can be written as

$$p^* = \frac{\dot{Q}}{4\mathscr{P}} \left\{ \Phi(\vec{r}) + \sum_{i=1}^{N} \frac{V}{\pi |\vec{r} - \vec{r}_i|} \right\}. \tag{19}$$

CYLINDRICAL SOLUTION

In the cylinder $\vec{r} = (r, \phi, z)$ is used as coordinate system. Since the cylinder is axisymmetric, the solution is independent of the angle ϕ. Therefore the Laplace operator is

$$\nabla^2 = \frac{1}{r} \frac{\partial}{\partial r} \left(r \frac{\partial}{\partial r} \right) + \frac{\partial^2}{\partial z^2} = \frac{\partial^2}{\partial r^2} + \frac{1}{r} \frac{\partial}{\partial r} + \frac{\partial^2}{\partial z^2}. \tag{20}$$

The field term of (19) can be written as $\Phi(r, z)$. $\Phi(r, z)$ is a solution of the equation $\nabla^2 \Phi = 4$, according to (5). In combination with (20) this leads to

$$\frac{\partial^2 \Phi}{\partial r^2} + \frac{1}{r} \frac{\partial \Phi}{\partial r} + \frac{\partial^2 \Phi}{\partial z^2} = 4. \tag{21}$$

An approximation of a general solution to (21) is

$$\Phi(r, z) = r^2 - R^2 \ln\left\{ \tfrac{1}{2}L + z + \sqrt{r^2 + \left(\tfrac{1}{2}L + z\right)^2} \right\}$$

$$- R^2 \ln\left\{ \tfrac{1}{2}L - z + \sqrt{r^2 + \left(\tfrac{1}{2}L - z\right)^2} \right\} + \sum_{n=1}^{M} C'_n F_n(r, z), \tag{22}$$

where r^2 is the particulate solution independent of z, the ln( ) terms are a correction for the decrease in the source term at the borders $\pm L/2$, the C'_n a series of coefficients to be determined from the boundary conditions (see next section), M is the number of C'_n constants, and

$$F_n(r, z) = \sum_{i=0}^{[\frac{1}{2}n]} y_{n,i} z^{n-2i} r^{2i}; \qquad y_{n,i} = \frac{\left(-\frac{1}{4}\right)^i n!}{(n-2i)!\,(i!)^2}. \tag{23}$$

In our simulations we found that the number of C'_n constants could be limited to five to obtain a satisfactory approximation.

Transformation of the generalized solution in (19) to cylindrical coordinates leads to

$$p^* = \frac{\dot{Q}}{4\mathscr{P}} \left\{ \Phi(r,z) + \sum_{i=1}^{N} \frac{V}{\pi\sqrt{r^2 + (z - z_i)^2}} \right\}. \tag{24}$$

FITTING OF HARMONIC FUNCTION

The calculated pO_2s at the locations of the erythrocytes have to match the pO_2 of the erythrocytes. Since the erythrocytes are not real point-like sources and do have volume, they are treated as spheres and the following interpretation of the erythrocyte pO_2 is used:

$$p_{\mathrm{E},i} = \frac{1}{2\pi} \int_{-\pi}^{\pi} d\varphi\, p(r_{\mathrm{E}}, \varphi, z_i), \tag{25}$$

where r_{E} is the radius of a sphere with the same volume as a erythrocyte. This means that the average pressure at $\vec{r} = (r_{\mathrm{E}}, \varphi, z_i)$ around the ith erythrocyte will be used as average erythrocyte rim pressure. Consequently, the same holds for $p^*_{\mathrm{E},i}$. Hence, when (24) is used, the oxygen driving force for erythrocyte i will be

$$p^*_{\mathrm{E},i} = p^*(r_{\mathrm{E}}, z_i) = \frac{\dot{Q}}{4\mathscr{P}} \left\{ \Phi(r_{\mathrm{E}}, z_i) + \sum_{j=1}^{N} \frac{V}{\pi\sqrt{r_{\mathrm{E}}^2 + (z_i - z_j)^2}} \right\}. \tag{26}$$

Since $p_{\mathrm{E},i}$ can be calculated with (16), the M constants C'_n in (22) can be fitted using least squares approximation. It turned out that $M = 5$ yields sufficiently accurate approximations.

EXTRACTION PRESSURE

When blood is modeled as a homogeneous fluid with an averaged heme concentration value, a pressure drop is used to account for the difference in behavior of homogeneous and heterogeneous blood. This pressure drop is called the extraction pressure [10, 11] or capillary barrier [12, 20]. For reasons stated by Hoofd [10] the term extraction pressure is used here. The extraction pressure (EP) is mathematically defined by

$$\mathrm{EP} = p_{r_{\mathrm{c}},\mathrm{he}} - p_{r_{\mathrm{c}},\mathrm{ho}}, \tag{27}$$

where $p_{r_c,\mathrm{he}}$ is the pO_2 at the capillary border at $z = z_i$ for heterogeneous blood and $p_{r_c,\mathrm{ho}}$ the pO_2 at the capillary border for homogeneous blood resulting in the same pO_2 at distant locations. Krogh published a formula for the calculation of the pressure drop from the capillary border into the tissue cylinder [15]. It was developed for tissue without myoglobin, but it can be applied directly for diffusion with facilitation [10]. With use of (6) the $p_{r_c,\mathrm{ho}}$ can be calculated by setting the pO_2 at the cylinder rim for homogeneous blood equal to that calculated for heterogeneous blood:

$$p^*_{r_c,\mathrm{ho}} = p^*_{\mathrm{R,he}} + \Delta p^*_{\mathrm{ho}}, \tag{28}$$

where

$$\Delta p^*_{\mathrm{ho}} = \frac{\dot{Q}}{4\mathscr{D}}\left\{-R^2 + r_c^2 + 2R^2 \ln\left(\frac{R}{r_c}\right)\right\}, \tag{29}$$

where Δp^*_{ho} is the difference in p^* at the capillary border and the tissue border for the homogeneous case.

RESULTS AND DISCUSSION

The major parameter concerning the particulate nature of blood is the hematocrit value. To investigate the effect of changes in hematocrit, the total oxygen supply has to be the same in all situations. Therefore the effects of different hematocrit values are considered at a constant product of blood flow and hematocrit. A similar investigation was done by Tsai and Intaglietta [19] using a numerical method. They developed a model with cylindrical erythrocytes and assumed steady-state kinetics for time intervals Δt in which the erythrocytes travel a distance equal to their length.

The parameter values used in the simulations are listed in Table 1. At high hematocrit values, the effect of pericapillary gradients as caused by the particulate nature will be lower than at low hematocrit values. This is obvious when the theoretical hematocrit value of 100% is used. In that case the capillary will be stuffed with erythrocytes in such a way that it becomes a homogeneous cylinder with erythrocyte contents. The physiologically interesting range of hematocrit is 20–50% [19]; therefore hematocrit values of 50, 30 and 20% are used. The simulations are visualized in graphs of the pO_2 against r and z. The formulas that were derived are only valid outside the erythrocytes.

Figure 2 shows simulations for three different hematocrit values. From this figure it can be seen that the oscillation in the pO_2 gradient

TABLE 1

Parameter Values for Various Simulations

	L [μm]	R [μm]	r_c [μm]	V_E [μm^3]	
Dimensional data	500†	10*	2.4*	66	
	$\mathscr{P}$ [mol m^{-1} kPa^{-1} s^{-1}]	$\dot{Q}$ [mol m^{-3} s^{-1}]	p_F [kPa]	$p_{50,Mb}$ [kPa]	
Tissue data	2.64×10^{-11}‡	0.665†	1.87*	0.71*	
	α_E [mol m^{-3} kPa^{-1}]	c_{Hm} [mol m^{-3}]	p_{50} [kPa]	n [−]	α_p [mol m^{-3} kPa^{-1}]
Blood data	1.17×10^{-2}‡	21.4†	4.93*	2.7†	$1.06\cdot10^{-2}$‡

		Figure				
		2a	2b	2c	3a	3b
Varying data	R [μm]	10	10	10	20	10
	$\dot{Q}$ [mol m^{-3} s^{-1}]	0.665	0.665	0.665	0.159	0.665
	p_a [kPa]	13.3	13.3	13.3	13.3	8.0
	F [m^3 s^{-1}]	2.4×10^{-14}	3.9×10^{-14}	5.8×10^{-14}	5.8×10^{-14}	5.8×10^{-14}
	H [−]	0.50	0.30	0.20	0.20	0.20
	Δz [μm]	7.25	12.2	17.9	17.9	17.9

*Data from Turek et al. [21].
†Data from Hoofd et al. [12].
‡Data from Clark et al. [2].

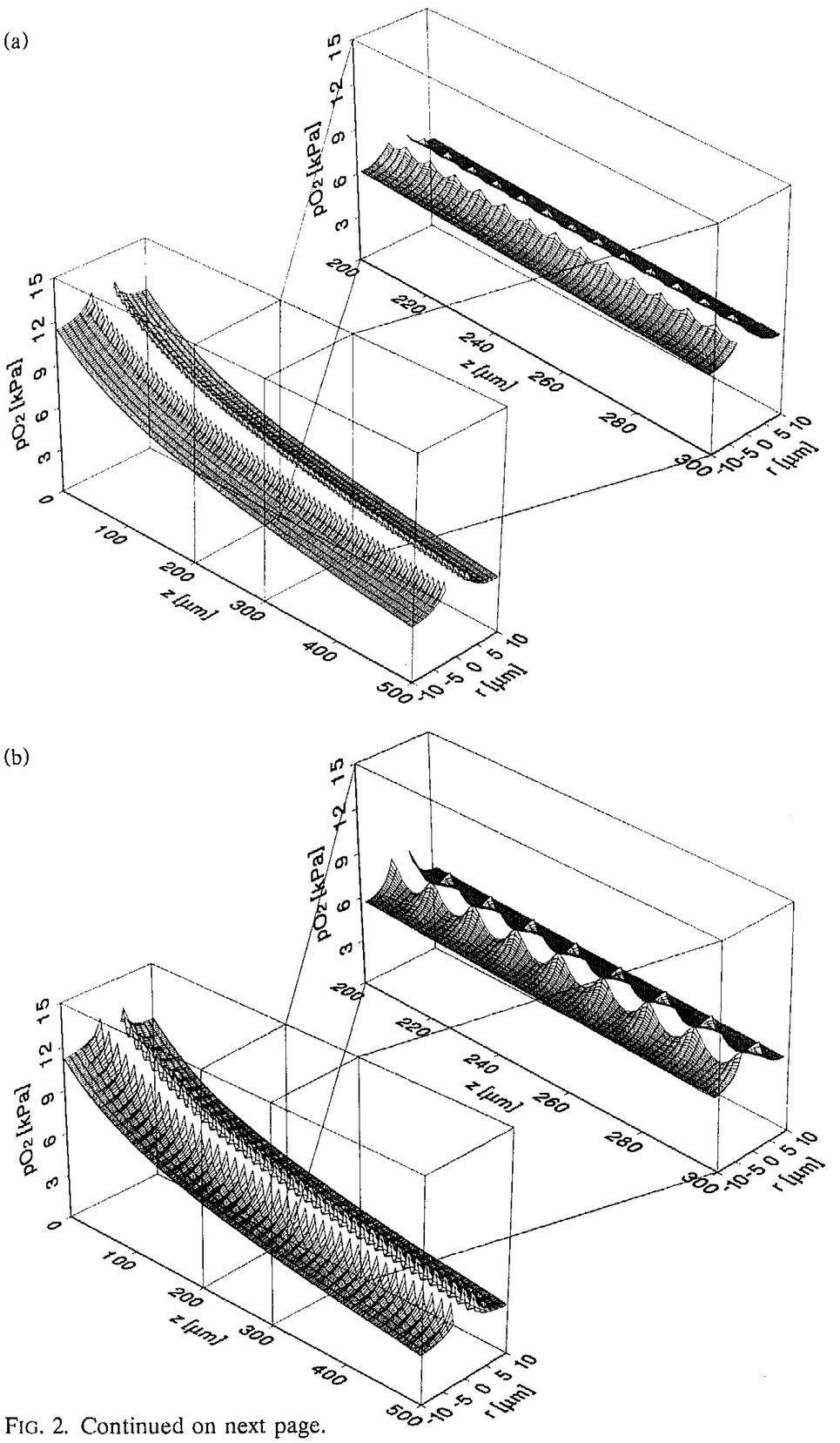

FIG. 2. Continued on next page.

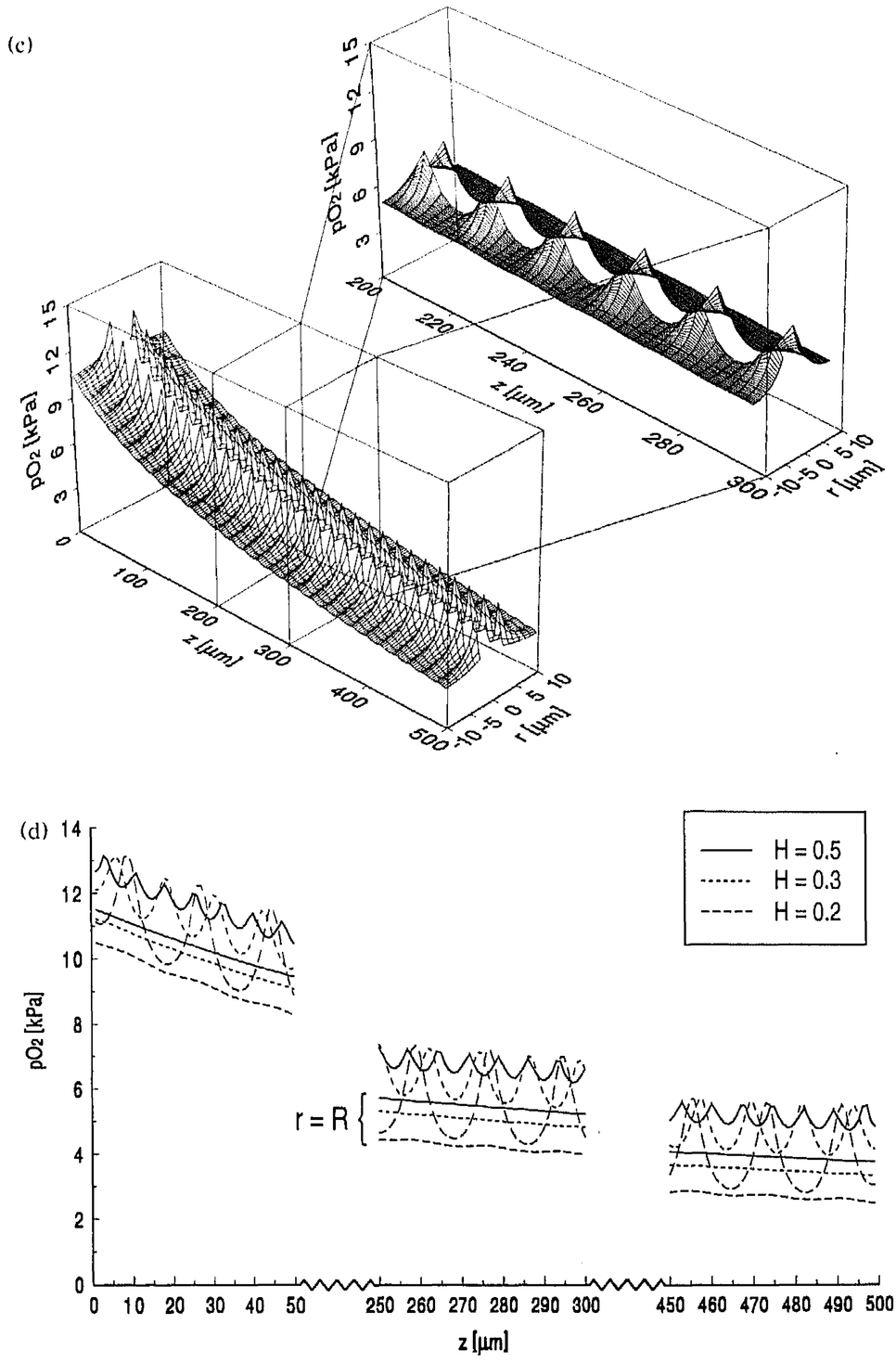

FIG. 2. Simulations for hematocrit values of (a) 50%, (b) 30%, and (c) 20%; close-ups are shown to get an impression of the pO_2-gradients involved. Additionally, in (d) the pO_2-gradients are shown at $r = r_c$ and $r = R$. Parameter values are listed in Table 1.

near the capillary fades out towards the tissue cylinder border and that the amplitude of the oscillations increases with decreasing hematocrit values. This is in accordance with expectation. For a hematocrit of 50% the amplitude decreases from 1.2 kPa at the capillary border to 0.01 kPa at the tissue cylinder rim, and for 20% the amplitude is reduced from 4.9 kPa to 0.2 kPa. In Figure 2c the pO_2 gradient is shown for a hematocrit value of 20%. In this case, the oscillations are still visible at the tissue border although they are much lower than at the capillary border. To investigate the disappearance of the oscillations at this hematocrit value, a simulation has also been done for a larger tissue cylinder radius. In order to compare both simulations at 20% hematocrit, an identical total oxygen consumption has been used in both tissue cylinders. This is obtained by setting the product of tissue volume and the oxygen consumption to a constant value. As can be seen in Figure 3, the amplitude has diminished considerably more, namely, from 1.6 at the capillary rim to 0.01 at the cylinder rim.

In some literature, a much lower arteriolar pO_2 is used, which contributes to a lower pO_2 in the tissue [7]. This will not have any effect on the amplitude on itself, as the oscillations are induced by the sum term of (24). When the tissue pO_2 drops to $p_{50,Mb}$, the oscillations are

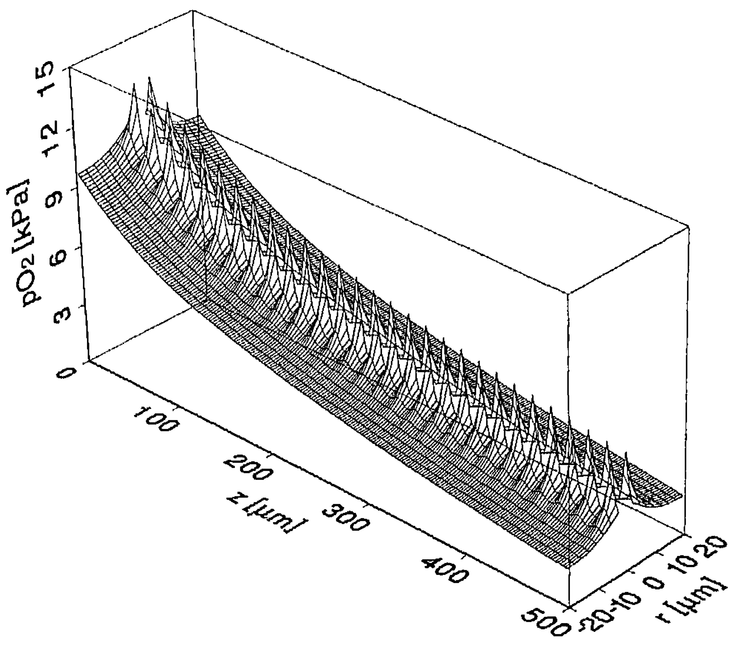

FIG. 3. Simulations for a hematocrit value of 20% with doubled tissue cylinder radius.

also damped by the facilitation since the oscillations are introduced in p^*, and it can be derived from (6) that the amplitude will at least be half of the amplitude without facilitation. When the arterial pO_2 is taken to be 8 kPa (60 mmHg) (not shown here) the leveling effect of the facilitation is not visible since hardly any decrease in amplitude can be seen compared to the normal pO_2 gradient along the tissue cylinder border at a hematocrit value of 20%. At the end of the capillary and at the cylinder rim, the amplitude is 0.11 kPa in this case compared to 0.15 kPa in Figure 2c.

In the hematocrit range chosen for the simulations, the oscillations have been reduced sufficiently to use the pO_2 at the cylinder border for calculation of the extraction pressure for homogeneous blood. As shown in Figure 4, the extraction pressure for the different hematocrit values ranges from 0.5 kPa to 2.6 kPa and is only slightly lower towards the venous end than at the arterial side. It should be noted that the extraction pressure found with the aid of the presented model results from the particulate nature only and is independent of the difference in oxygen transport in the capillary and the tissue.

The EP is meant to correct the assumption of homogeneous blood; however, one has to be careful in applying this assumption to blood with low hematocrit values. Federspiel and Sarelius [5] found that blood is homogeneous with respect to oxygen supply at hematocrit values as low

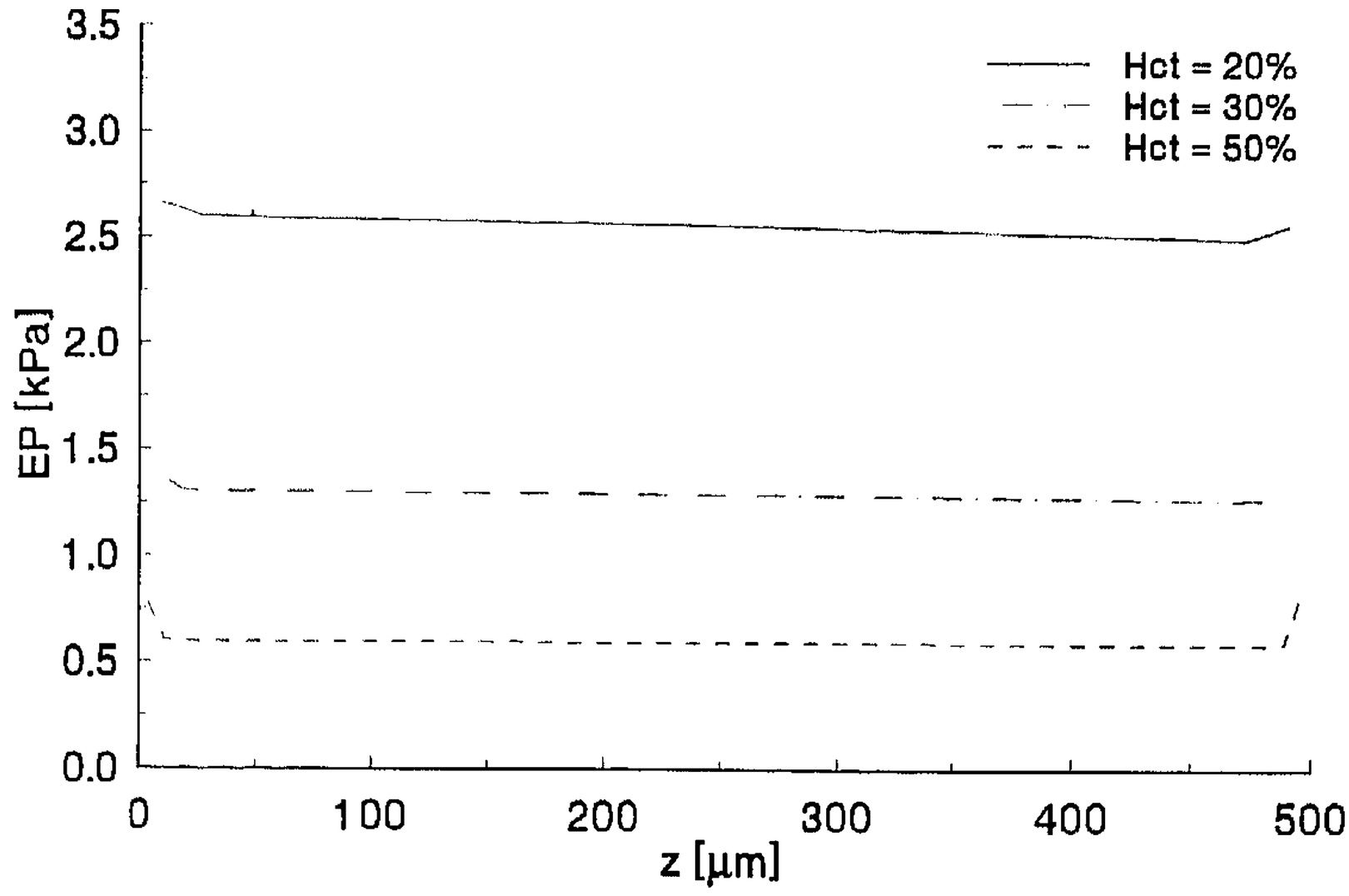

FIG. 4. Extraction pressure (EP) along the cylinder for simulations with different hematocrit values.

as 20% at low oxygen consumption, i.e., resting muscle. In working muscle the blood was found to be homogeneous only for hematocrit values of about 50%. Additionally, Groebe and Thews [8] concluded for maximally working skeletal muscle 'that non-uniformity of the oxygen flux out of the capillaries due to large inter-erythrocytic plasma gaps does not play an important role for tissue oxygen supply as long as average red blood cell spacing is sufficiently small to guarantee an appropriate overall capillary oxygen flux.' Hellums [9] investigated the effect of the discrete cell treatment compared to the continuum treatment by means of a change in resistance. He found an increased resistance for the discrete cell treatment. Federspiel and Popel [4] developed a model for the oxygen transport in the capillaries where blood was treated as a two-phase medium and they showed that the capillary mass transfer coefficient depends on the spacing and the clearance (R/r_e) of the particles in the capillary. They found an increased resistance for increased spacing, which is expressed in this study as an increased EP. The clearance does not play a role in the present study since the plasma is not incorporated in the model.

Tsai and Intaglietta [18] found that at a hematocrit value of 20% an empirically based distribution of sources yields the same levels of oxygenation as an even spacing. Therefore, the combination of EP values and the assumption of homogeneous blood is probably valid for hematocrit values as low as 20%. Lower hematocrit values can cause an unevenly spaced system to behave differently at erythrocyte trails and at the gaps within the erythrocyte trails, resulting in different EP values depending on the local erythrocyte spacing.

CONCLUSIONS

In the literature different models have been presented that describe parts of the oxygen transport to muscle tissue. All those models have their own objectives and most of them can roughly be divided into two major groups: one describing the oxygen transport in and close to at most a few capillaries and thus taking into account the particulate nature of blood, and one describing full tissue oxygenation—many capillaries—with the assumption of homogeneous blood. The model presented here extends the latter class of models to heterogeneous blood by estimating the EP. This model is used as a basis for the calculation of the EP results in similar pO_2 gradients as those obtained by Tsai and Intaglietta [19].

It is shown here that the modeling of erythrocytes as point-like sources can be used to estimate the EP. At physiologically valid ranges

of parameter choices, a pO_2 gradient at the tissue cylinder rim in the z direction is found comparable to the gradient for Krogh-like solutions. The oscillations in the pO_2 gradient generated by the erythrocytes have an amplitude that depends strongly on the hematocrit value and tissue radius, and, to a lesser extent, also on the facilitation of oxygen transport by myoglobin. The effect of the first two parameters can be explained by their relation to the support volume since the oscillating part of the equations depends on this volume. The decrease in amplitude caused by the facilitation can be explained by the leveling effect of the facilitation on pO_2 at low pO_2 values.

The EP not only depends on capillary parameters such as the hematocrit and the capillary radius, but also on tissue parameters such as the tissue volume supplied by one erythrocyte, the permeability, and the oxygen consumption rate. For a given set of parameters, the EP is almost constant throughout the tissue cylinder length; hence it can easily be used as a constant in calculations involving the Krogh equations. In this way the estimations for the oxygenation level of different tissues regions can be enhanced. At low hematocrit values, however, one has to be careful when treating blood as a homogeneous medium.

APPENDIX A: VALIDATION OF STROBOSCOPE APPROACH

The use of a stroboscope approach is based on the assumption of quasi-steady state. This assumption applied to (4) results in the assumption $\partial c_{O_2}/\partial t = 0$. This is normally only true for $\tau_D \ll \tau_v$, where τ_D is the characteristic time for diffusion and τ_v is the characteristic time for the velocity of the erythrocytes. These are defined as

$$\tau_D = \frac{a^2}{D}; \qquad \tau_v = \frac{a}{v}, \tag{A1}$$

where a is a characteristic distance to be found from the distances of the system. There are two distances involved, the erythrocyte spacing Δz and the blood/tissue interface at $r = r_c$ so that a presumably is a combination of these two.

Both blood and tissue separately are stationary systems; the time-dependent phenomena originate from the interface. When an erythrocyte passes by, local tissue boundary conditions are different from when a plasma gap passes by. Single erythrocytes can be discerned only for $\Delta z > 0$, or better when the individual sources are distinct. That implies that the analysis can be focused on the part of (24) that is ascribed to

the sources:

$$\sum_{i=1}^{N} \frac{1}{\sqrt{r^2 + (z - z_i)^2}}. \tag{A2}$$

In Figure 5 it is shown that without the sum term no oscillations can be found and that the contribution of the sum term is only the oscillations. Equation (A2) can be considered as resulting from a stroboscope flash at time $t = 0$ and the corresponding nonsteady extension around that moment is found replacing z by $z - vt$. 'Around that moment' can be specified as $-\frac{1}{2}\Delta t < t < \frac{1}{2}\Delta t$, where $\Delta z = v\,\Delta t$. We have to consider the time-dependent nonsteady extension at $r = r_c$ which we will denote by Σ having dimension length^{-1}:

$$\Sigma = \sum_{i=1}^{N} \frac{1}{\sqrt{r_c^2 + (z - vt - z_i)^2}}. \tag{A3}$$

Verification of the assumption $\partial c_{O_2} / \partial t = 0$ now comes down to showing that $\partial \Sigma / \partial t$ is small, i.e., (much) smaller than the other terms in the differential equation, notably

$$\left| \frac{\partial \Sigma}{\partial t} \right| \ll \left| D \frac{\partial^2 \Sigma}{dz^2} \right|. \tag{A4}$$

When worked out, this results in

$$\left| \sum_{i=1}^{N} \frac{v(z - vt - z_i)}{\left\{ r_c^2 + (z - vt - z_i)^2 \right\}^{3/2}} \right| \ll \left| D \sum_{i=1}^{N} \frac{2(z - vt - z_i)^2 - r_c^2}{\left\{ r_c^2 + (z - vt - z_i)^2 \right\}^{5/2}} \right|, \tag{A5}$$

where an appropriate value of $z - vt$ has to be chosen at either side of the inequality. In terms of characteristic times, the left side can be interpreted as $(a'\tau_v)^{-1}$ and the right side as $(a'\tau_D)^{-1}$, where a' is a representational distance, and (A4), (A5) come down to the inequality $\tau_D \ll \tau_v$. We will choose the distance a' equal to r_c. Equation (A5) should be worked out in the middle part of a large array which can be

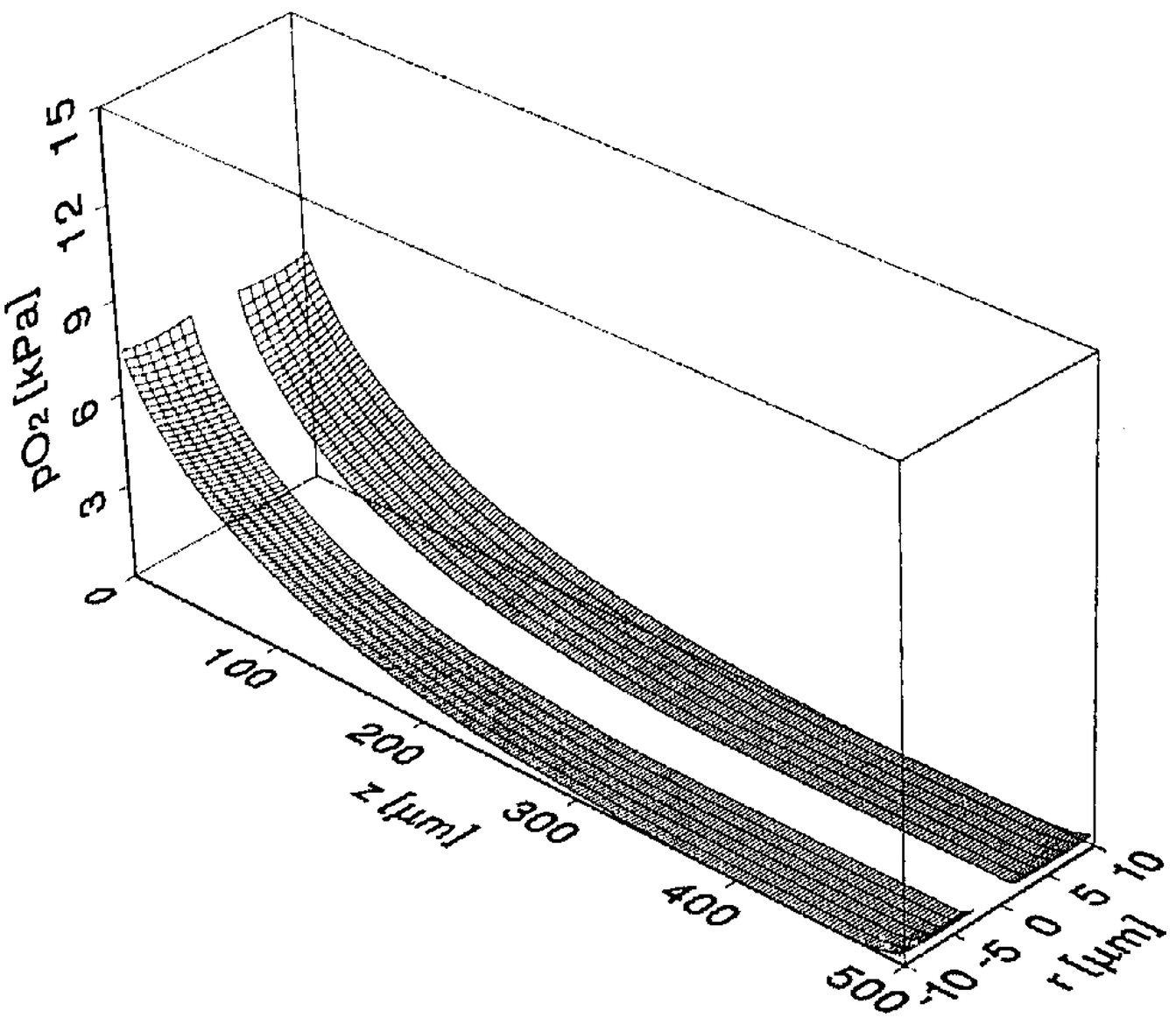

(a)

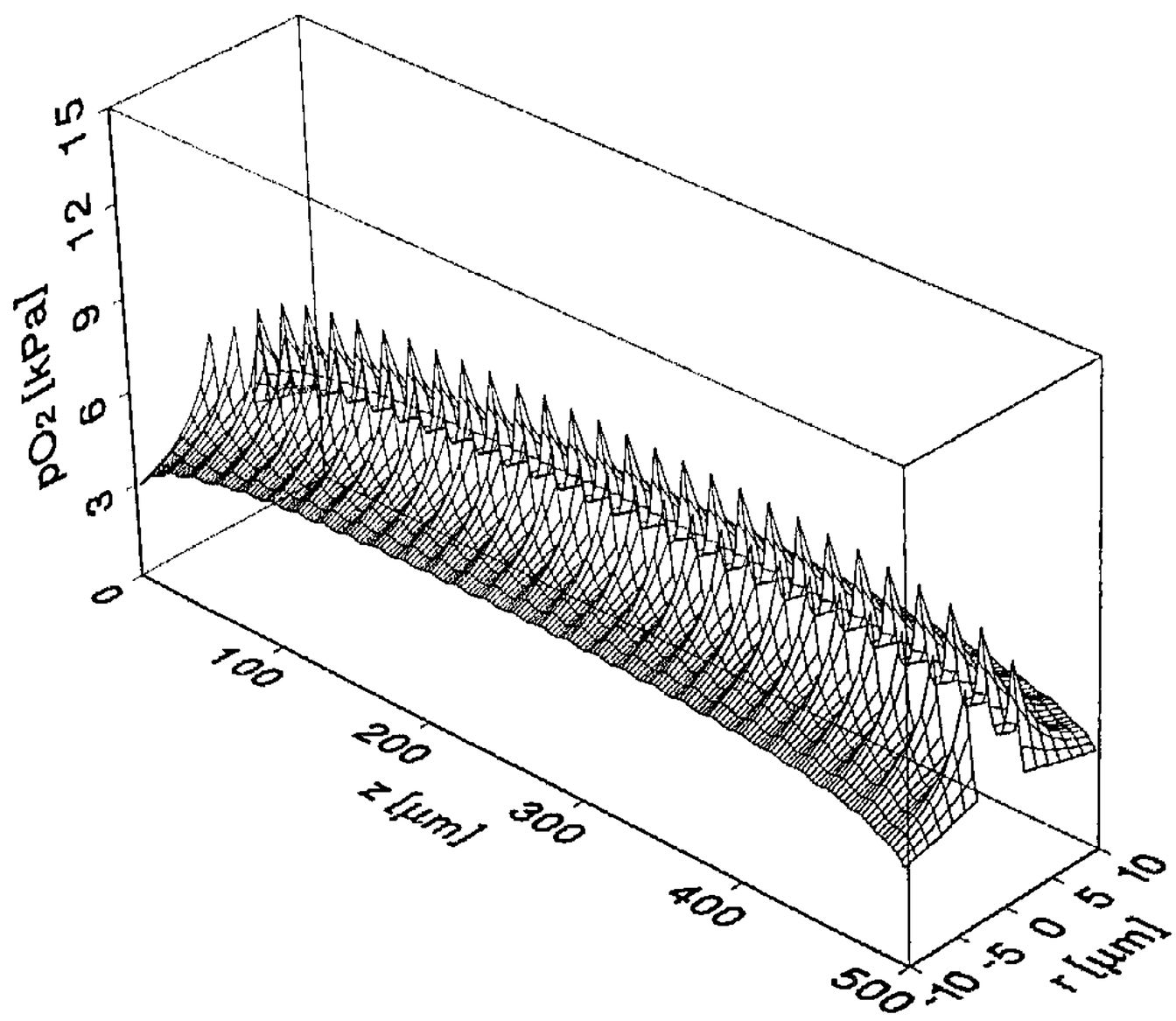

(b)

FIG. 5. Contribution of the different terms of (24) to the pO_2 gradient with (a) only the $\Phi(r, z)$ term and (b) only the sum term.

done by extending the summation to i: $-\infty \rightarrow +\infty$ and choosing a value of $z - vt$ between $-\frac{1}{2}\Delta z$ and $+\frac{1}{2}\Delta z$ so that we can take $z_i = i\,\Delta z$.

Because of its symmetry, the evaluation of the right-hand term of (A5) at $z - vt = 0$ to determine τ_D is straightforward:

$$\frac{1}{\tau_D} = Dr_c \sum_{i=-\infty}^{\infty} \frac{r_c^2 - 2i^2\Delta z^2}{\{r_c^2 + i^2\Delta z^2\}^{5/2}} = \frac{D}{r_c^2} g_D(\Delta z / r_c), \qquad \text{(A6)}$$

where the function g_D is defined to represent the summation in terms of the dimensionless fraction $\Delta z / r_c$. The left-side term of (A5) is antisymmetric and therefore yields zero at $z - vt = 0$; or, better, at $z - vt = \frac{1}{2}k\,\Delta z$ for any integer value of k. Therefore, it seems reasonable to choose a value in between, $z - vt = \frac{1}{4}\Delta z$ for the evaluation of τ_v:

$$\frac{1}{\tau_v} = v\,\Delta z r_c \sum_{i=-\infty}^{\infty} \frac{i + \frac{1}{4}}{\left\{r_c^2 + \left(i + \frac{1}{4}\right)^2 \Delta z^2\right\}^{3/2}} = \frac{v}{r_c} g_v(\Delta z / r_c) \qquad \text{(A7)}$$

with a similar definition of g_v. These characteristic times can be worked out for the cases here, where only a limited number of terms around $i = 0$ has to be evaluated because the above formulas are estimates and the sum terms decrease as i^{-3} and i^{-2}, respectively. The relevant fraction that has to be small is

$$\tau_D / \tau_v = \frac{v r_c}{D} \frac{g_v(\Delta z / r_c)}{g_D(\Delta z / r_c)}. \qquad \text{(A8)}$$

Obviously, this quantity linearly depends on v so that the stroboscope method will be valid at least in the limit $v \rightarrow 0$. For the influence of Δz and r_c, the quotient g_v / g_D has to be considered which depends on the quotient of these two. Two regimes are important: small and large $\Delta z / r_c$. For $\Delta z \rightarrow 0$, the sources come so close that they can no longer be discerned individually and the capillary blood looks homogeneous. Accordingly, in Figure 4 EP is found to approach zero. From the same figure the other regime, large Δz, is seen to be more interesting. It is easily derived that $g_D \rightarrow 1$, $g_v \rightarrow 0$ in the limit for $\Delta z / r_c \rightarrow \infty$, or, better

for g_v:

$$g_v(X) \underset{X \to \infty}{\to} \frac{16}{X^2} \sum_{k=0}^{\infty} \frac{(-1)^k}{(2k+1)^2} \approx \frac{14.7}{X^2} \tag{A9}$$

so that the stroboscope method also will be valid for large Δz:

$$\Delta z^2 \gg 14.7 \frac{v}{D} r_c^3. \tag{A10}$$

For the data used here this implies $\Delta z^2 \gg (8.3\ \mu\text{m})^2$. The cases considered here mostly do not fall within these low- and high-Δz restraints, but is seems more important that the stroboscope approach is expected to be valid for both small and large Δz and consequently might be considered a valuable first-order approximation also for the remaining range of Δz values. Anyhow, it is expected to be a good approximation for low velocities v.

APPENDIX B: LIST OF SYMBOLS

C'_n	constants in the field term Φ
$c_{E,i}$	total amount of oxygen in erythrocyte i
c_{Hm}	hem concentration
c_{Mb}	concentration of deoxymyoglobin
c_{O_2}	total amount of oxygen per volume
c_{O_2Mb}	concentration of oxymyoglobin
D_{O_2Mb}	diffusivity of oxymyoglobin
EP	extraction pressure
F	blood flow
F_n	parameter in the field term Φ
H	capillary hematocrit
i	source number
J	flux of oxygen and oxymyoglobin
J_{O_2}	oxygen flux based on diffusion
J_{O_2Mb}	flux of oxymyoglobin
L	length of capillary
M	number of C'_n constants used
N	number of sources
n	Hill coefficient
n_i	oxygen contained in plasma and erythrocyte at source i
p	oxygen partial pressure
p^*	oxygen diffusion driving quantity

p_0^*	integration constant
$p_{R,\mathrm{he}}^*$	oxygen driving force at tissue cylinder wall for heterogeneous case
$p_{r_c,\mathrm{ho}}^*$	oxygen driving force at capillary wall for homogeneous blood
p_{50}	pO_2 at which hemoglobin is 50% saturated
$p_{50,\mathrm{Mb}}$	pO_2 at which myoglobin is 50% saturated
p_a	pO_2 at the arterial side of the capillary
$p_{r_c,\mathrm{he}}$	pO_2 at capillary wall at $z = z_i$ for heterogeneous blood
$p_{r_c,\mathrm{ho}}$	pO_2 at capillary wall at $z = z_i$ for homogeneous blood
$p_{\mathrm{E},i}$	pO_2 inside erythrocyte i
p_F	facilitation pressure
$p_{\mathrm{p},i}$	mean pO_2 in plasma at erythrocyte i
pO_2	oxygen partial pressure
Δp_ho^*	difference in p^* at capillary and tissue cylinder rim for homogeneous blood
$\Delta p_{\mathrm{E},p}$	difference between erythrocyte and plasma pO_2
$\dot{Q}$	oxygen consumption
R	radius of tissue cylinder
$\vec{r}$	cylindrical or spherical coordinate
r_c	radius of capillary
r_E	radius of fictitious spherical erythrocyte
$\vec{r}_i$	location of the ith source
s	hemoglobin saturation
s_i	hemoglobin saturation in erythrocyte i
s_Mb	myoglobin saturation
t	time
Δt	time needed for a source to travel the distance Δz
V	cylinder volume/number of erythrocytes
v	velocity of sources
V_E	erythrocyte volume
V_p	plasma volume in V
V_T	tissue volume of tissue supplied by one erythrocyte
z	axial coordinate
z_i	axial coordinate of the ith source
Δz	distance between two successive sources
α_E	oxygen solubility in erythrocyte
α_p	oxygen solubility in plasma
y	parameter in F_n
Φ	field term

ρ	distance from centre in spherical coordinate system
$\vec{\nabla}$	gradient operator
∇^2	Laplace operator
$\mathscr{P}$	permeability

REFERENCES

1 P. T. Baxley and J. D. Hellums, A simple model for simulation of oxygen transport in the microcirculation, *Ann. Biomed. Engrg.* 11:401–416 (1983).

2 A. Clark Jr., W. J. Federspiel, P. A. Clark, and G. R. Cokelet, Oxygen delivery from red cells, *Biophys. J.* 47:171–181 (1985).

3 H. Degens, Z. Turek, L. J. C. Hoofd, M. A. van't Hof, and R. A. Binkhorst, The relationship between capillarisation and fibre types during compensatory hypertrophy of the plantaris muscle in the rat, *J. Anat.* 180:455–463 (1992).

4 W. J. Federspiel, and A. S. Popel, A theoretical analysis of the effect of the particulate nature of blood on oxygen release in capillaries, *Microvasc. Res.* 32:164–189 (1986).

5 W. J. Federspiel, and I. H. Sarelius, An examination of the contribution of red cell spacing to the uniformity of oxygen flux at the capillary wall, *Microvasc. Res.* 27:273–285 (1984).

6 J. E. Fletcher, Mathematical modeling of the microcirculation, *Math. Biosci.* 38:159–202 (1978).

7 K. Groebe, A versatile model of steady state O_2 supply to tissue. Application to skeletal muscle, *Biophys. J.* 57:485–498 (1990).

8 K. Groebe and G. Thews, Effects of the red cell spacing and red cell movement upon oxygen release under conditions of maximally working skeletal muscle, *Adv. Exp. Med. Biol.* 248:175–185 (1989).

9 J. D. Hellums, The resistance to oxygen transport in the capillaries relative to that in the surrounding tissue, *Microvasc. Res.* 13:131–136 (1977).

10 L. Hoofd, Updating the Krogh model—assumptions and extensions, in *Oxygen Transport in Biological Systems*, Society for Experimental Biology Seminar Series 51, S. Egginton and H. F. Ross, eds., Cambridge University Press, Cambridge, 1992, pp. 197–229.

11 L. Hoofd, J. Olders, and Z. Turek, Oxygen pressures calculated in a tissue volume with parallel capillaries, *Adv. Exp. Med. Biol.* 277:21–29 (1990).

12 L. Hoofd, Z. Turek, and J. Olders, Calculation of oxygen pressures and fluxes in a flat plane perpendicular to any capillary distribution, *Adv. Exp. Med. Biol.* 248:187–196 (1989).

13 B. Klitzman, A. S. Popel, and B. R. Duling, Oxygen transport in resting and contracting hamster cremaster muscles: Experimental and theoretical microvascular studies, *Microvasc. Res.* 25:108–131 (1983).

14 F. Kreuzer, Oxygen supply to tissues: The Krogh model and its assumptions, *Experientia* 38:1415–1426 (1982).

15 A. Krogh, The number and distribution of capillaries in muscles with calculations of the oxygen pressure head necessary for supplying the tissue, *J. Physiol.* 52:409–415 (1919).

16 A. S. Popel, Diffusion in tissue slices with metabolism obeying Michaelis–Menten kinetics, *J. Theor. Biol.* 80:325–332 (1979).
17 A. S. Popel, Theory of oxygen transport to tissue, *Crit. Rev. Biomed. Engrg.* 17:257–321 (1989).
18 A. G. Tsai and M. Intaglietta, Local tissue oxygenation by statistically distributed sources, *Microvasc. Res.* 44:200–213 (1992).
19 A. G. Tsai and M. Intaglietta, Local tissue oxygenation during constant red blood cell flux: A discrete source analysis of velocity and hematocrit changes, *Microvasc. Res.* 37:308–322 (1989).
20 Z. Turek, J. Olders, L. Hoofd, S. Egginton, F. Kreuzer, and K. Rakusan, pO_2 histograms in various models of tissue oxygenation in skeletal muscle, *Adv. Exp. Med. Biol.* 248:227–237 (1989).
21 Z. Turek, K. Rakusan, J. Olders, L. Hoofd, and F. Kreuzer, Computed myocardial pO_2 histograms: Effects of various geometrical and functional conditions, *J. Appl. Physiol.* 70:1845–1853 (1991).
22 C.-H. Wang and A. S. Popel, Effect of red blood cell shape on oxygen transport in capillaries, *Math. Biosci.* 116:89–110 (1993).